Review of Scientific Instruments

RESEARCH ARTICLE | NOVEMBER 06 2014

Study of electrical conductivity response upon formation of ice and gas hydrates from salt solutions by a second generation high pressure electrical conductivity probe

Barbara Sowa; Xue Hua Zhang; Karen A. Kozielski; Dave E. Dunstan; Patrick G. Hartley; Nobuo Maeda

Rev. Sci. Instrum. 85, 115101 (2014)
https://doi.org/10.1063/1.4900658

AIP Publishing

Study of electrical conductivity response upon formation of ice and gas hydrates from salt solutions by a second generation high pressure electrical conductivity probe

Barbara Sowa,[1,2] Xue Hua Zhang,[3] Karen A. Kozielski,[4] Dave E. Dunstan,[2] Patrick G. Hartley,[1] and Nobuo Maeda[1,a)]

[1]*CSIRO Materials Science and Engineering, Ian Wark Laboratory, Bayview Avenue, Clayton, VIC 3168, Australia*
[2]*Department of Chemical and Biomolecular Engineering, School of Engineering, University of Melbourne, VIC 3010, Australia*
[3]*School of Civil, Environmental and Chemical Engineering, RMIT University, Melbourne 3001, Australia*
[4]*CSIRO Earth Science and Resource Engineering, Ian Wark Laboratory, Bayview Avenue, Clayton, VIC 3168, Australia*

(Received 19 June 2014; accepted 18 October 2014; published online 6 November 2014)

We recently reported the development of a high pressure electrical conductivity probe (HP-ECP) for experimental studies of formation of gas hydrates from electrolytes. The onset of the formation of methane-propane mixed gas hydrate from salt solutions was marked by a temporary upward spike in the electrical conductivity. To further understand hydrate formation a second generation of windowless HP-ECP (MkII), which has a much smaller heat capacity than the earlier version and allows access to faster cooling rates, has been constructed. Using the HP-ECP (MkII) the electrical conductivity signal responses of NaCl solutions upon the formation of ice, tetrahydrofuran hydrates, and methane–propane mixed gas hydrate has been measured. The concentration range of the NaCl solutions was from 1 mM to 3M and the driving AC frequency range was from 25 Hz to 5 kHz. This data has been used to construct an "electrical conductivity response phase diagrams" that summarize the electrical conductivity response signal upon solid formation in these systems. The general trend is that gas hydrate formation is marked by an upward spike in the conductivity at high concentrations and by a drop at low concentrations. This work shows that HP-ECP can be applied in automated measurements of hydrate formation probability distributions of optically opaque samples using the conductivity response signals as a trigger. [http://dx.doi.org/10.1063/1.4900658]

INTRODUCTION

Gas hydrates or clathrate hydrates have been the subject of intense scientific and industrial research for some time since they have been suggested as gas storage media, and as a potential energy source.[1] The formation of gas hydrates can also be problematic for some applications such as flow assurance in natural gas pipelines.[2] It is thus of great interest to understand hydrate formation probability distributions under given experimental conditions. The challenge is that the measurements of induction time at a constant subcooling (a common measure of hydrate formation probability) are very time consuming and the results highly stochastic.[5] A different approach is therefore required for the experimental establishment of hydrate formation probability distributions.

To this end a High Pressure Automated Lag Time Apparatus (HP-ALTA) for flow assurance applications has recently been developed.[3] The physical principles of HP-ALTA are based on an ambient pressure version of ALTA developed earlier.[4] The instrument can experimentally measure gas hydrate formation probability distributions by subjecting a sample to >100 of linear cooling ramps and recording the hydrate formation temperature, T_f. The use of linear cooling ramps effectively keeps increasing the driving force for hydrate formation until nucleation is forcibly induced. This protocol effectively compresses the long and highly stochastic induction time distributions at a constant subcooling temperature to more compact maximum achievable subcooling distributions.[5] The typically deep subcoolings that are achieved in a HP-ALTA causes the growth of the hydrate phase in the forms of films at the aqueous–gas interface to take place rapidly once the nucleation barrier is surmounted.[6]

The HP-ALTA was used to study the effect of gas pressures, cooling rate, and gas composition as reported previously.[7] An empirical equation that relates the induction time at a constant subcooling to T_f during a linear cooling ramp was also developed in a prior study.[5] Most recently, the utility of the HP-ALTA was demonstrated by applying the instrument for inhibition efficacy ranking of a batch of kinetic hydrate inhibitors (KHIs) and for the quantification of the so called memory effect in those systems.[8]

There are several limitations in the HP-ALTA technologies, however. The most important is that the use of optical techniques renders it unsuitable for the study of optically opaque samples. In addition, HP-ALTA is unsuitable for the study of surfactant solutions (common hydrate promoters[9–11]). Dissociation of gas hydrates after each cooling cycle causes formation of bubbles (because the solubility of non-polar gases in water is low), and the presence of

a)Nobuo.Maeda@csiro.au

surfactants stabilizes these bubbles which continue to scatter light and prevent measurements of subsequent runs.

In order to overcome the experimental problems relating to bubbles, a high pressure electrical conductivity probe (we refer to this first generation of the instrument as HP-ECP MkI) for experimental studies of formation of gas hydrates from electrolytes was developed.[12] We note at this stage that electrolytes (salts) are thermodynamic hydrate inhibitors (THIs)[13] and that brine is encountered in sea bed sediments and in deep sea natural gas pipelines, especially in aged fields.[14,15] In HP-ECP MkI, the onset of the formation of methane-propane mixed gas hydrate from 2M NaCl solution was marked by a temporary upward spike in the electrical conductivity. Likewise, the onset of the formation of ice from 1M NaCl solution was also marked by an upward spike in the electrical conductivity. It was also observed that the sharpness of the spike depended on the AC frequency used for the measurement and that the optimum AC frequency for the best signal to noise (S/N) ratio depended on the concentration of the electrolyte.[12] However, the details of the interdependence are yet to be examined.

HP-ECP MkI was equipped with two high pressure windows to allow visual inspection of an electrolyte sample together with the monitoring of the electrical conductivity signal.[12] However, the bulky design of HP-ECP MkI rendered its heat capacity large and hence limited the maximum accessible cooling rate during a cooling ramp to 0.005 K/s. Consequently, each experiment was highly time-consuming, even with the use of linear cooling ramps.

In this work the use of the second generation of the high pressure electrical conductivity probe (we refer to this instrument as HP-ECP MkII) is reported. MkII inherits the advantage of the MkI which is the capacity to detect hydrate formation in optically opaque samples. However, unlike MkI, MkII is window-less and its more compact design allowed the use of faster cooling rates during cooling ramps. To demonstrate the capability of HP-ECP MkII, we systematically studied the electrical conductivity changes of NaCl solutions upon the formation of ice, *tetrahydrofuran (THF)* model hydrates, and methane–propane (C1/C3) mixed gas hydrate.

MATERIALS AND METHODS

HP-ECP MkII

Figure 1 shows the schematic description of the HP-ECP MkII. The pressure chamber is made of stainless steel (approximately 40 mm × 30 mm × 45 mm). The chamber is pressure rated up to 15 MPa. The pressure chamber is sandwiched between two Peltier devices (Peltier-CP1.4-127-06L-RTV, Melcor) of approximately 40 mm × 40 mm each, which in turn are sandwiched between two custom made aluminum heat sinks. The heat sinks have channels inside them so that they can be cooled using an appropriate coolant such as an alcohol or glycol. The coolant is cooled and circulated by an external refrigerated bath (Model WCR-P12, All-Lab Scientific). The chamber is also equipped with a thermometer (PT100 HEL705, Honeywell) that is placed at a reference point in the chamber block, approximately 5 mm away from

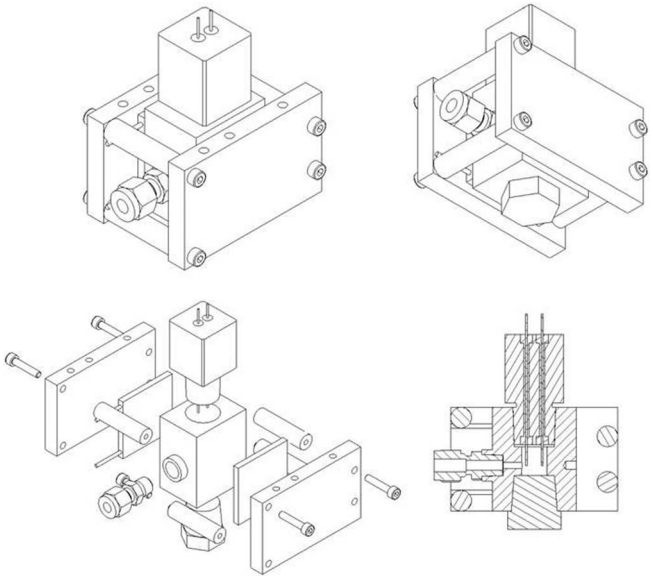

FIG. 1. Schematic description of the HP-ECP MkII. The basic features and the operating principles are the same as the original version of the HP-ECP.[12] To reduce the heat capacity of the chamber and speed up measurements, the two high pressure windows that had been present in the earlier version of the HP-ECP were eliminated.

the centre of the chamber (the thermometer is under ambient pressure). This thermometer reading is output to a PC, which also allows feedback control of the current to the Peltier devices.

The conductivity probe is made of two platinum wires of 0.8 mm diameter (99.95%, A&E Metal Merchants, Marrickville, NSW, Australia) 7.5 mm apart, and goes into the high pressure chamber vertically from the top. Epoxy Araldite was used to fill the gap between the platinum wire and the 2.5 mm diameter vertical through hole of the stainless steel block for electrical insulation. The epoxy araldite was 53 mm thick along the vertical dimension of the hole and it adequately withstood the pressure of up to 15 MPa. A spring with a weak spring constant was placed at the bottom of the chamber and a glass sample cell (approximately 5 mm in diameter and 10 mm in height) was placed on top of the spring. This configuration ensures that the ends of the two platinum wires are in contact with the bottom of the glass sample cell during an experiment while protecting the platinum wires from being bent. The liquid level of a sample electrolyte is adjustable but we only used the depth of 5 mm in the current study to allow for systematic comparison.

Custom written software (Labview, version 8.5, National Instruments) is used to measure and control the temperature of the sample using the thermometer and Peltier inputs/outputs. The same software also records the electrical conductivity of the sample. AC voltage of 200 mV in amplitude and a selection from a range of 25 Hz–10 kHz in frequency can be applied to the sample.

A series of calibration measurements were carried out to (1) calculate the temperature of the sample inside the chamber from the temperature reading from the thermometer which sit about 5 mm away, (2) find the required electric current supply to the Peltier devices to control the temperature of the

sample to desired values. A calibration factor which relates the thermometer temperature response to the actual sample temperature was derived from control experiments using another thermometer immersed in ethanol in the sample cell within the sample chamber (under atmospheric pressure). Another series of control experiments was carried out to calculate the electric current that is required to ensure that the Peltier device maintained the temperature of the sample cell at a specified value. Within the physical constraints of this hardware (i.e., the heat capacity of the chamber and the power of the Peltier device), the instrument could cool the sample at a constant (linear) cooling rate of up to 0.05 K/s.

Once the sample cell is in place, the high pressure gas line is connected to the HP-ECP MkII using a $\frac{1}{4}''$ Swagelok connector (SS-400-1-2, Swagelok, Broadmeadows, Australia). The methane–propane (C1/C3) mixed gas (90 mol. % methane and 10 mol. % propane) was purchased from BOC and used as received. We note at this stage that C1/C3 mixed gas forms a Structure II (sII) hydrate.[2] The gas cylinder regulator of a desired gas is opened and a pressure booster pump (Model AG-62, Haskel Australasia Pty Ltd, Queensland, Australia) is activated to pressurize the instrument to a desired value.

While the gas pressure in the system stabilizes, the refrigerated bath is switched on and the temperature is usually set to 268 K. The electronics and the computer are switched on and the program is activated. At this point, the gas cylinder is isolated from the pressure line, and the pressure booster pump is switched off for safety reasons. Pressure transducers in the pressure line allow continued monitoring of gas pressure in the system for the duration of the measurements.

Measurements of the formation of ice and THF hydrate at ambient pressure

For the study of ice and THF hydrates which does not require elevated pressures, a simple probe constructed from two platinum wires and that can be fitted onto an NMR-type glass tube of an ambient pressure version of the automated lag time apparatus was used (ALTA-A). Briefly, an essentially identical set of control software and electronics were installed for ALTA-A, and appropriate calibration measurements were carried out. This modified ALTA-A allows electrical conductivity measurements of formation of ice and THF hydrate at ambient pressure and simultaneous monitoring of the optical transmittance through the electrolyte in the so-called "bulk transmittance configuration."[3] Unlike HP-ECP MkII, the ends of the platinum wires in ALTA-A are not in contact with the bottom of the sample cell. Rather, the window for the optical measurement is placed approximately 9 mm above the bottom of the glass sample cell (3 mm below the ends of the platinum wires).[12] Approximately 200 μl of the salt solution was cooled at a constant rate of 0.05 K/s until the formation of ice or THF hydrate.

Aqueous solutions of sodium chloride between 1 mM to 3M were selected for the study. The Milli-Q water (resistivity >18.2 MΩ) was used for the preparation of all samples and cleaning the glassware. Sodium chloride was purchased from MERCK and purified by re-crystallization. For the samples that involve tetrahydrofuran (THF), the liquid mixture of THF (MERCK; 99.9%) and water (MilliQ-water) with a stoichiometry of 1:17 fraction (19 wt. % THF) was used for all samples. For a salt solution that involves THF, the molar ratio of THF to H_2O was maintained at 1:17 in each case.

RESULTS AND DISCUSSION

Types of electrical conductivity signal response upon formation of ice and gas hydrates

Figures 2–4 show examples of the electrical conductivity signal response upon formation of (1) ice, (2) THF hydrate, and (3) C1/C3 mixed gas hydrate in the measurement by MkII. The driving AC frequency used in these specific examples was 100 Hz and 2.5 kHz for ice, 5 kHz, and 2.5 kHz for the THF hydrate and 25 Hz and 5 kHz for the mixed gas hydrate systems, as shown in the figure captions. We started a cooling ramp from 295 K for the ice and the THF hydrate formation measurements and from 310 K for the C1/C3 mixed gas hydrate formation measurements. These starting temperatures ensure complete dissociation of ice/gas hydrates and avoid the memory effect. In the results presented below, however, we do not show the whole range of the results. We omit the high temperature section of the results, which do not contain any significant events, to provide details of the temperature regions of interest.

As the temperature decreased from 290 K to 265 K in NaCl solutions (Figure 2), the conductivity gradually

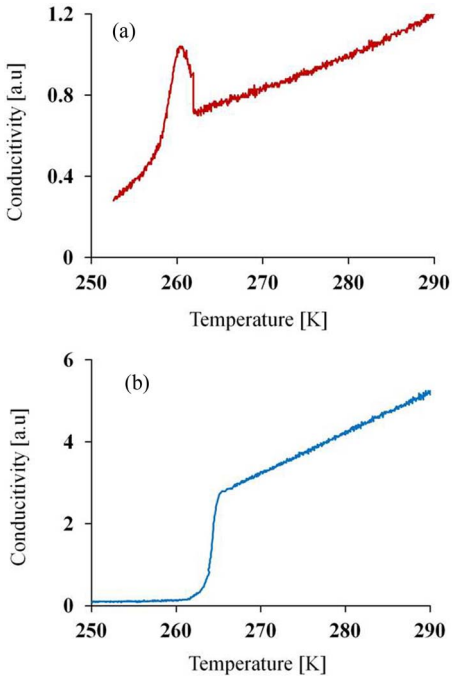

FIG. 2. Example electrical conductivity profiles of NaCl solutions in the ambient pressure during a cooling ramp. The cooling rate was 0.05 K/s. (a) A temporary increase in the conductivity ("spike") was observed upon formation of ice for the concentrated solutions (red). In the example shown, the concentration was 0.1M and the AC driving frequency was 100 Hz. (b) A drop in the conductivity ("drop") was observed for more dilute solutions (blue). In the example shown, the concentration was 0.01M and the AC driving frequency was 2.5 kHz.

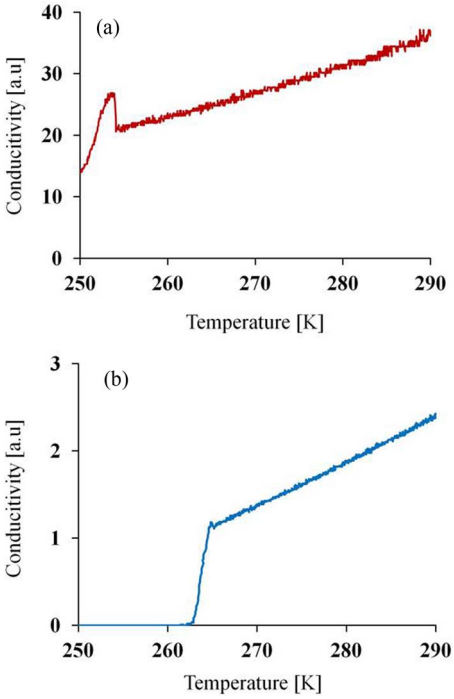

FIG. 3. Example electrical conductivity profiles of NaCl–THF mixed solutions in the ambient pressure during a cooling ramp. The cooling rate was 0.05 K/s. (a) A temporary increase in the conductivity ("spike") was observed upon formation of THF hydrate for the concentrated solutions (red). In the example shown, the NaCl concentration was 1M and the AC driving frequency was 5 kHz. (b) A drop in the conductivity ("drop") was observed for more dilute solutions (blue). In the example shown, the NaCl concentration was 0.001M and the AC driving frequency was 2.5 kHz.

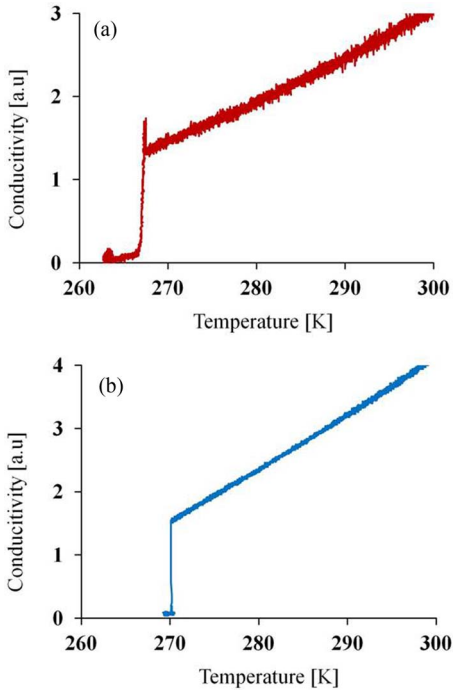

FIG. 4. Example electrical conductivity profiles of NaCl solutions in the atmosphere of 7.7 MPa of C1/C3 mixed gas during a cooling ramp. The cooling rate was 0.005 K/s. (a) A temporary increase in the conductivity ("spike") was observed upon formation of C1/C3 mixed gas hydrate for rather concentrated solutions (red). In the example shown, the NaCl concentration was 0.1M and the AC driving frequency was 25 Hz. (b) A drop in the conductivity ("drop") was observed for more dilute solutions (blue). In the example shown, the NaCl concentration was 0.001M and the AC driving frequency was 5 kHz.

decreased. Likewise, the conductivity of THF aqueous solution gradually decreased as it cooled from 290 K to 265 K (Figure 3). The conductivity of NaCl solutions in pressurized C1/C3 mixed gas atmosphere also decreased as it cooled from 300 K to 270 K (Figure 4). Therefore in each system, the electrical conductivity decreased with cooling prior to a phase transition,[16,17] which is consistent with the previous report.[12] Such gradual decrease in conductivity is due to the increase in the viscosity of the aqueous solution with cooling;[18,19] the mobility of the ions in the solution falls accordingly.

With further cooling, a sudden change in the electrical conductivity was eventually observed, which was attributed to the formation of ice or gas hydrate. ALTA-A monitored and recorded both the intensity of the transmittance light through the sample and the electrical conductivity, as reported earlier.[12] The sudden change in the electrical conductivity signal occurred simultaneously when the transmittance light intensity dropped sharply.[12] This event marked the formation of ice or THF hydrate. For C1/C3 mixed gas hydrate, HP-ECP MkII is windowless and its formation cannot be independently visually confirmed. Nevertheless, HP-ECP MkI allowed visual inspection of the sample and the formation of gas hydrate was visible after the detection of conductivity spike.[12] Here we assume that the electrical conductivity signal response in HP-ECP MkII also corresponded to the formation of C1/C3 mixed gas hydrate.

Ice formation occurred around 262 K in 0.1M NaCl solution (Figure 2(a)) and around 265 K in 0.01M NaCl solution (Figure 2(b)). Figure 3 shows that THF hydrate formed around 254 K in 1M NaCl solution (Figure 3(a)) and around 264 K in 0.001M NaCl solution (Figure 3(b)). Likewise, Figure 4 shows that C1/C3 mixed gas hydrate formed around 268 K in 0.1M NaCl solution (Figure 4(a)) and around 270 K in 0.001M NaCl solution (Figure 4(b)).

Detailed examination of the data showed that there were two different types of electrical conductivity signal responses upon formation of ice or gas hydrates: a temporary increase followed by a decrease (we call it a "spike" hereafter) shown in Figures 2(a) and 3(a), and 4(a) (each coloured with red) or a decrease without a "spike" (we call it a "drop" hereafter) shown in Figures 2(b) and 3(b), and 4(b) (each coloured with blue).

Sometimes it was difficult to determine if a transition was marked by a drop or by a very small spike. For example, it is unclear if there was a tiny spike before a sharp drop in Figure 3(b). We classified such change that was comparable in magnitude to the noise level at the end of the linear cooling as a "drop."

It remains unclear at this stage what physical mechanisms cause the appearance of a spike or a drop at particular combinations of salt concentrations and driving frequencies.[12] In order to be able to use these types of electrical conductivity response signal as a trigger for automated measurements, we decided to explore how the types of signals was related to the concentration of the salt solutions and the optimal driving AC frequency that yields the best S/N ratio. We expanded our study of these electrical conductivity signal responses in MkII measurements to cover a wider range of electrolyte concentration and the driving AC frequency. We then constructed a map

or an "electrical conductivity response signal phase diagram" for each system.

Electrical conductivity signal response "phase diagram" upon formation of ice and gas hydrates

Figures 5–7 summarize the electrical conductivity response signal upon formation of (1) ice, (2) THF hydrate, and (3) C1/C3 mixed gas hydrates, respectively. In each diagram, the abscissa shows the selected electrolyte concentration and the ordinate shows the selected driving AC frequency. Note that the scale is not linear in either coordinate. We first sealed a selected concentration of NaCl solution in HP-ECP MkII and pressurized with C1/C3 mixed gas. Then we selected the driving frequency to one of the values shown in Figures 5–7. Once the driving frequency was selected, the sample was subjected to a linear cooling ramp. The sample was kept being cooled until some conductivity response signal was observed. Then the sample was manually heated to 310 K for 300 s. The conductivity signal recovered to the original value after this heating. The measurement was then repeated 4 or 5 times for each set of selected electrolyte concentration and the driving AC frequency. Figure 8 shows an example of such repeated measurements for the case of 1M NaCl and the AC frequency of 1 kHz. As can be seen, the repeatability within these 4 or 5 repeat runs under the same experimental conditions was good.

In Figures 5–7, the region in which a "spike" was observed upon transition is mapped with red and the region in which a "drop" was observed is mapped with blue. It can be seen that there was a trend that a spike was commonly observed at higher salt concentrations whereas a drop was commonly observed at lower salt concentrations, for each system. As noted above, it is possible that the presence of a very small spike that was comparable in magnitude as the noise level was ignored. This uncertainty may somewhat shift the boundary of the "phases," but the basic trend remains the same.

We found that the spike at a higher concentration was easier to observe than that at a lower concentration at the same

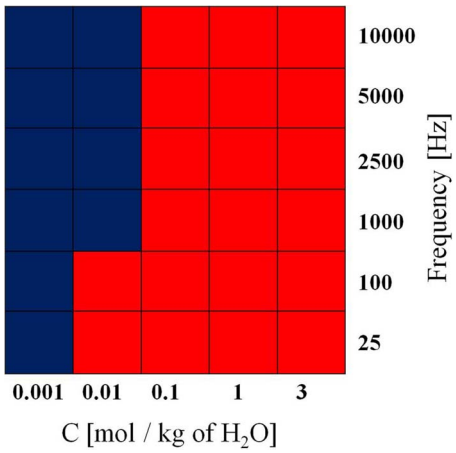

FIG. 5. "Electrical conductivity response phase diagram" upon formation of ice from NaCl solutions of a range of concentrations. A temporary increase in the conductivity ("spike") was observed upon formation of ice for rather concentrated solutions (red region). A drop in the conductivity ("drop") was observed for more dilute solutions (blue region).

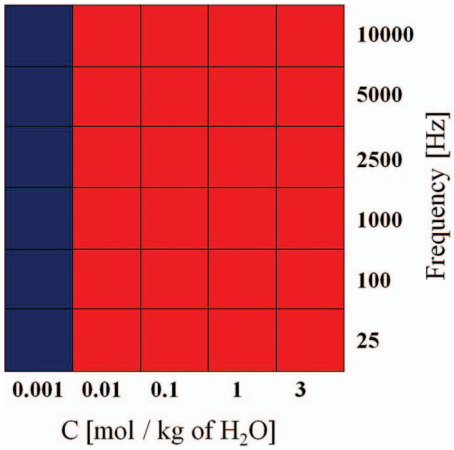

FIG. 6. "Electrical conductivity response phase diagram" upon formation of THF hydrate from NaCl solutions of a range of concentrations. A temporary increase in the conductivity ("spike") was observed upon formation of ice for rather concentrated solutions (red region). A drop in the conductivity ("drop") was observed for more dilute solutions (blue region).

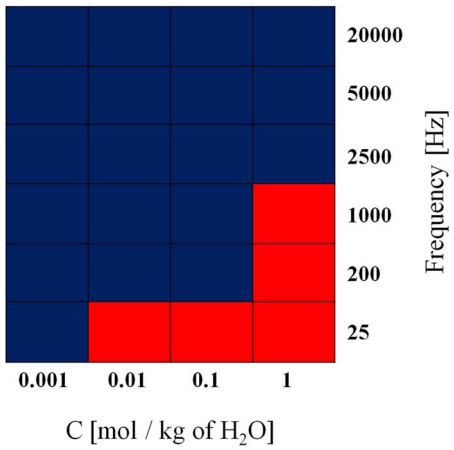

FIG. 7. "Electrical conductivity response phase diagram" upon formation of C1/C3 mixed gas hydrate from NaCl solutions of a range of concentrations under an atmosphere of C1/C3 mixed gas at 7.8 MPa. A temporary increase in the conductivity ("spike") was observed upon formation of ice for rather concentrated solutions (red region). A drop in the conductivity ("drop") was observed for more dilute solutions (blue region).

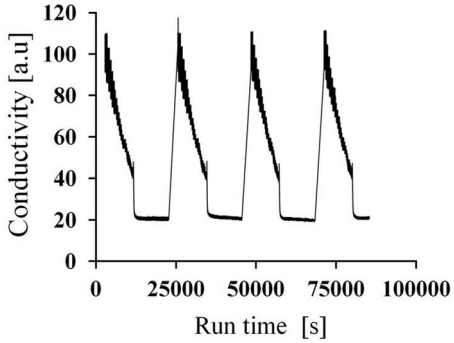

FIG. 8. An example which shows good repeatability within the 4 to 5 repeat runs under the same experimental conditions. This particular example is for C1/C3 mixed gas hydrate formation at 7.8 MPa of the C1/C3 mixed gas pressure. The NaCl concentration was 1M and the AC driving frequency was 1kHz. In each of the four cooling ramps a spike was observed immediately prior to a sharp drop in the electrical conductivity.

frequency. However, we could not find a good method to normalize the size of a spike. For example, the absolute magnitude of a spike was clearly greater the greater the concentration. On the other hand, the relative magnitude of a spike as a percentage of the conductivity value of the base (immediately prior to the "spike" event) was clearly greater the lower the concentration (and hence the normalization factor in the denominator was small). As such, below we only confine ourselves to more qualitative distinctions.

When a "spike" was observed, the electrical conductivity then either came down to a smaller but clearly non-zero value or came down all the way to virtually zero (below the sensitivity of the instrument). The former was observed at high salt concentrations. The latter was observed at low salt concentrations.

Similarly, when a "drop" was observed, the electrical conductivity then either dropped to a smaller but clearly non-zero value or came down all the way to virtually zero (below the sensitivity of the instrument). Once again, the former was observed at high salt concentrations. The latter was observed at low salt concentrations.

If an additional "phase" is assigned to each of "a spike followed by a drop to a non-zero value," "a spike followed by a drop to zero," "a drop to a non-zero value," and "a drop to zero," then the phase diagrams for ice, THF hydrate, and C1/C3 mixed gas hydrate become Figures 9–11, respectively.

These observations are complex and difficult to explain, as multiple factors may be simultaneously at play. First, we consider the effect of electrolyte concentration. One possible factor is that the presence of NaCl, a thermodynamic hydrate inhibitor (THI), inhibits the growth of the C1/C3 mixed gas hydrate. Heterogeneous nucleation of gas hydrate is likely to occur at the container wall at the three-phase line, and then the hydrate may grow away from the wall toward the centre of the sample cell. This process could increase the concentration of the salt in the liquid section of the sample, including where the platinum probes are located. If the growth rate of the C1/C3 mixed gas hydrate slows down with increasing NaCl concentration, then the presence of NaCl may slow the drop of electrical conductivity. For dilute solutions for which the growth inhibition effect is insignificant, electrical conductivity drops more readily.

There may be several other factors, but here we merely note that (1) gas hydrate itself is an insulator, (2) gas hydrate will exclude ions as it forms (that is why it can be applied for desalination[1,20]), (3) this ion exclusion would cause the electrolyte concentration in the unconverted part of the sample to increase, (4) formation of ice is also known to exclude ions from its lattice, albeit to a lesser extent.[21–23] The solubility of NaCl in water is significantly higher than the concentration range we studied, even at the lowest temperature studied,[24] so we can preclude the possibility of precipitation of NaCl due to cooling.

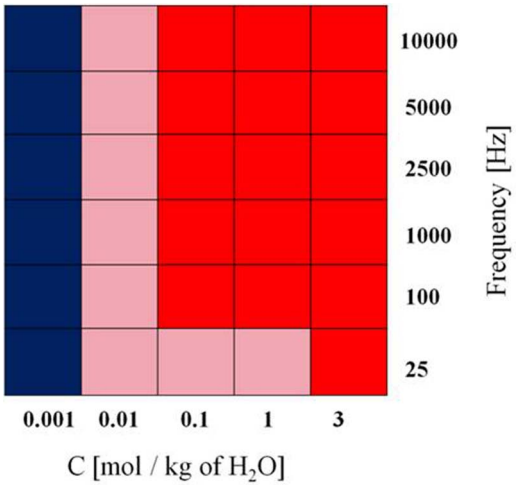

FIG. 10. A more detailed version of the "Electrical conductivity response phase diagram" upon formation of THF hydrate from NaCl solutions shown in Figure 6. "Spike followed by a drop to non-zero conductivity" (dark red), "spike followed by a drop to zero conductivity" (light red), "drop to non-zero conductivity" (light blue), "drop to zero conductivity" (dark blue).

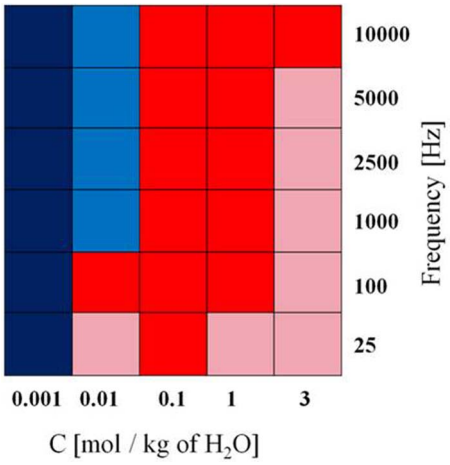

FIG. 9. A more detailed version of the "Electrical conductivity response phase diagram" upon formation of ice from NaCl solutions shown in Figure 5. "Spike followed by a drop to non-zero conductivity" (dark red), "spike followed by a drop to zero conductivity" (light red), "drop to non-zero conductivity" (light blue), "drop to zero conductivity" (dark blue).

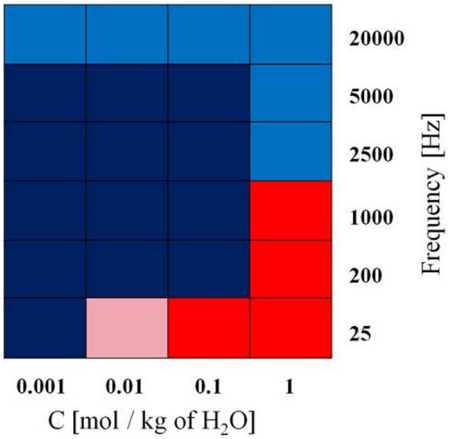

FIG. 11. A more detailed version of the "Electrical conductivity response phase diagram" upon formation of C1/C3 mixed gas hydrate from NaCl solutions at 7.8 MPa shown in Figure 7. "Spike followed by a drop to non-zero conductivity" (dark red), "spike followed by a drop to zero conductivity" (light red), "drop to non-zero conductivity" (light blue), "drop to zero conductivity" (dark blue).

We now consider the effect of driving AC frequency. We observe from Figures 5 and 6 that there was only a very weak trend, if any, in relation to the driving AC frequency for the ice and the THF hydrate systems. There may be a weak trend that the higher the driving AC frequency the electrical conductivity response was more likely to be a drop than a spike. This trend was much more pronounced for C1/C3 mixed gas hydrate formation, however, as shown in Figure 7.

The pronounced trend observed for C1/C3 mixed gas hydrate formation may be surprising given the limited range of experimentally accessible driving frequency. The amount of ions that is being excluded from a unit volume of aqueous solution upon the formation of C1/C3 mixed gas hydrate is somehow decreasing with increasing driving frequency. It could become more difficult for the ions to respond to the more rapidly oscillating electric field in a timely manner. Then some ions that would have escaped to the continuous bulk portion of the unconverted phase may be trapped within the grain boundaries of hydrate crystals and no longer contribute to the electrical conductivity measured by HP-ECP.

Control experiments that demonstrate the reliability of HP-ECP technology

It is conceivable that the presence of Pt wire provides heterogeneous nucleation sites for gas hydrate formation and shifts the measured C1/C3 mixed gas hydrate formation probability distributions. To investigate this effect, we first show the effect of the presence of platinum (Pt) wire on the formation probability distribution of C1/C3 mixed gas hydrates. These control experiments were carried out by using HP-ALTA. The Pt wire used here was from the same source as the Pt wires used in the conductivity probe of HP-ECP. A short Pt wire (<1 cm) was placed at the edge of a sample cell in a HP-ALTA so that the wire was out of the optical path and part of the wire was protruding through the water/gas surface, as is the case in a HP-ECP. Figure 12 shows the T_f distribution of the sample of water with and without Pt wire. The results are

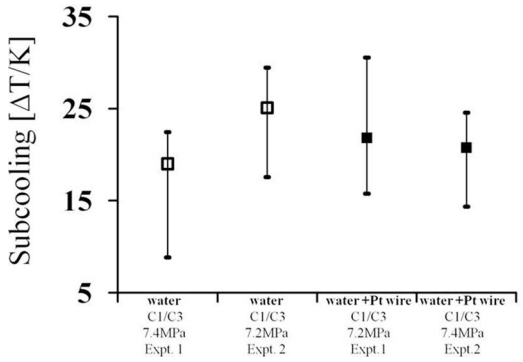

FIG. 12. The effects of Pt wire on the formation probability distributions at selected gas pressure for the control purposes. The open/closed symbols show the most probable T_f values which were calculated using the CPDF method[8] of C1/C3 mixed gas hydrates in pure water. Pt wire was placed at the edge of a "boat" of HP-ALTA. The following conditions were used here: cooling rate 0.025 K/s; heating temperature after each cooling ramp, $T = 310$ K; heating time, $t = 300$ s. The "error bars" indicate the full width of experimentally measured "stochasticity."[7]

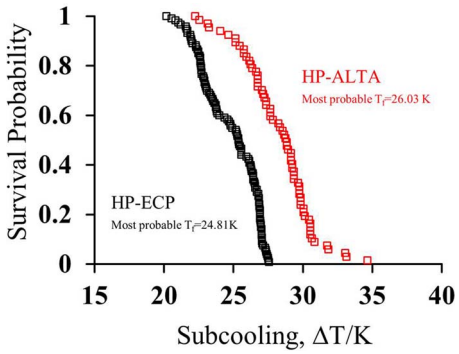

FIG. 13. The formation probability distributions of C1/C3 mixed gas hydrates in 0.001M NaCl at 7MPa, using both HP-ALTA (red symbols) and HP-ECP (black symbols) for control purposes. The most probable T_f values calculated from the respective CPDF were 24.81 K and 26.03 K, respectively.

expressed in the form of the most probable T_f (open symbols)[8] and the "stochasticity" (which appears like an error bar in Figure 12).[3,7] The most probable T_f was calculated from the Cumulative Probability Distribution Function (CPDF) of gas hydrate formation.[8] It can be seen that the presence of Pt wire did not shift the T_f of gas hydrates significantly compared to that in pure water without Pt wire.

We now show example automated experiments by HP-ECP (MkII). For the control purposes, we use an electrically conductive but also optically transparent NaCl solution here, so that the results can be compared to the results using HP-ALTA. Figure 13 shows the S-Curves of C1/C3 mixed gas hydrate formation in 0.001M NaCl measured using HP-ECP (MkII) and HP-ALTA. Our results showed that the T_f distributions obtained using both HP-ALTA and HP-ECP were overlapping, albeit there may be a slight bias toward lower T_f (greater subcooling) for those measured using HP-ALTA. Given that the presence of Pt wire alone did not cause any appreciable shift in the T_f distributions (see above), this slight bias could be a result of the presence of electric current in HP-ECP (but not in HP-ALTA).

CONCLUSIONS AND FUTURE STUDY

A second generation HP-ECP (MkII) instrument which has a much smaller heat capacity than the earlier version is reported. Using HP-ECP MkII the electrical conductivity signal responses of NaCl solutions upon the formation of ice, THF model hydrates, and methane–propane mixed gas hydrate has been studied in detail. It is observed that the electrical conductivity signal responses depended on the concentration of the electrolytes and, to a lesser extent, to a choice of driving AC frequency. Therefore, in the future studies on gas hydrate formation by using HP-ECP the effect of frequency may be dismissed.

Based on the knowledge gained in this study, we can now select an appropriate type of response signal to detect gas hydrate formation for automated measurements. The control automated experiments using electrically conductive and transparent NaCl solution showed that the C1/C3 mixed gas hydrate formation probability distribution measured using HP-ECP is similar to that measured using HP-ALTA. The

HP-ECP technology has not been applied in the study of gas hydrates in different systems before. Our view is that our results presented here serve as a baseline for the future work. We observed a high potential of that technology to examine opaque substances and their effect of gas hydrate formation. We can now extend our investigation to the study of gas hydrate formation probability distributions of cationic and anionic surfactant solutions, which are well known hydrate promoters.

ACKNOWLEDGMENTS

This work was supported by the Australian Research Council Future Fellowship (FT0991892) and CSIRO's Energy Flagship.

[1]P. Englezos, "Clathrate hydrates," Ind. Eng. Chem. Res. **32**, 1251–1274 (1993).
[2]E. D. Sloan and C. A. Koh, *Clathrate Hydrates of Natural Gases*, 3rd ed. (CRC Press, Boca Raton, 2008).
[3]N. Maeda, D. Wells, N. C. Becker, P. G. Hartley, P. W. Wilson, A. D. J. Haymet, and K. A. Kozielski, "Development of a high pressure automated lag time apparatus for experimental studies and statistical analyses of nucleation and growth of gas hydrates," Rev. Sci. Instrum. **82**, 065109 (2011).
[4]A. F. Heneghan, P. W. Wilson, G. M. Wang, and A. D. J. Haymet, "Liquid-to-crystal nucleation: Automated lag-time apparatus to study supercooled liquids," J. Chem. Phys. **115**, 7599–7608 (2001).
[5]R. Wu, K. A. Kozielski, P. G. Hartley, E. F. May, J. Boxall, and N. Maeda, "Probability distributions of gas hydrate formation," AIChE J. **59**, 2640–2646 (2013).
[6]R. Wu, K. A. Kozielski, P. G. Hartley, E. F. May, J. Boxall, and N. Maeda, "Methane-propane mixed gas hydrate film growth on the surface of water and Luvicap EG solutions," Energy Fuels **27**, 2548–2554 (2013).
[7]N. Maeda, D. Wells, P. G. Hartley, and K. A. Kozielski, "Statistical analysis of supercooling in fuel gas hydrate systems," Energy Fuels **26**, 1820–1827 (2012).
[8]E. F. May, R. Wu, M. A. Kelland, Z. M. Aman, K. A. Kozielski, P. G. Hartley, and N. Maeda, "Quantitative kinetic inhibitor comparisons and memory effect measurements from hydrate formation probability distributions," Chem. Eng. Sci. **107**, 1–12 (2014).
[9]N. Ando, Y. Kuwabara, and Y. H. Mori, "Surfactant effects on hydrate formation in an unstirred gas/liquid system: An experimental study using methane and micelle-forming surfactants," Chem. Eng. Sci. **73**, 79–85 (2012).
[10]K. Okutani, Y. Kuwabara, and Y. H. Mori, "Surfactant effects on hydrate formation in an unstirred gas/liquid system: An experimental study using methane and sodium alkyl sulfates," Chem. Eng. Sci. **63**, 183–194 (2008).
[11]Y. Zhong and R. E. Rogers, "Surfactant effects on gas hydrate formation," Chem. Eng. Sci. **55**, 4175–4187 (2000).
[12]N. Maeda, "Development of a high pressure electrical conductivity probe for experimental studies of gas hydrates in electrolytes," Rev. Sci. Instrum. **84**, 015110 (2013).
[13]Y. Qi, W. Wu, Y. Liu, Y. Xie, and X. Chen, "The influence of NaCl ions on hydrate structure and thermodynamic equilibrium conditions of gas hydrates," Fluid Phase Equilib. **325**, 6–10 (2012).
[14]J.-W. Jung and J. C. Santamarina, "Hydrate formation and growth in pores," J. Cryst. Growth **345**, 61–68 (2012).
[15]X. Zang, D. Liang, and N. Wu, "Gas hydrate formation in fine sand," Sci. China: Earth Sci. **56**, 549–556 (2013).
[16]Y. C. Wu and W. F. Koch, "Absolute determination of electrolytic conductivity for primary standard kcl solutions from 0-degrees-c to 50-degrees-c," J. Solution Chem. **20**, 391–401 (1991)
[17]K. W. Pratt, W. F. Koch, Y. C. Wu, and P. A. Berezansky, "Molality-based primary standards of electrolytic conductivity - (IUPAC technical report)," Pure Appl. Chem. **73**, 1783–1793 (2001).
[18]M. Hayashi, "Temperature-electrical conductivity relation of water for environmental monitoring and geophysical data inversion," Environ. Monit. Assess. **96**, 119–128 (2004).
[19]R. A. Robinson and R. H. Stokes, *Electrolyte Solutions* (Butterworths, London, 1965).
[20]P. Kyeong-Nam, H. Sang Yeon, L. Jin Woo, K. Kyung Chan, L. Young Cheol, H. Myung-Gyu, and L. Ju Dong, "A new apparatus for seawater desalination by gas hydrate process and removal characteristics of dissolved minerals (Na +, Mg 2+, Ca 2+, K +, B 3+)," Desalination **274**, 91–96 (2011).
[21]V. F. Petrenko and R. W. Whitworth, *Physics of Ice* (Oxford University Press, Oxford, 1999).
[22]G. W. Gross, P. M. Wong, and K. Humes, "Concentration dependent solute redistribution at ice-water phase boundary. III. Spontaneous convection-chloride solutions," J. Chem. Phys. **67**, 5264–5274 (1977).
[23]P. W. Wilson and A. D. J. Haymet, "Workman-Reynolds freezing potential measurements between ice and dilute salt solutions for single ice crystal faces," J. Chem. Phys. B **112**, 11750–11755 (2008).
[24]*CRC Handbook of Chemistry and Physics*, 80th ed., edited by D. R. Lide (CRC Press, Boca Raton, 1999).